

## ABSTRACT

This study involves the preparation of fine alumina powders derived from Bayer gibbsite and also aqueous alumina suspensions by using tri block copolymers. Preparation of alumina powders was performed by decomposition of gibbsite into transition alumina phase followed by controlled transformation to alpha phase. To increase transformation rate to  $\alpha$ -alumina in transition phase hence influence the nucleation and growth rate of the solid-solid phase transformation ball milling and ultrasonication was applied. Gibbsite was thermally treated at 900 °C to reach a transition form of alumina. In some cases a heat treatment at 350 °C was applied to create a network of submicroscopic cracks in the heated gibbsite that may help grinding. Ball milling and ultrasonic treatment before calcination at 1100, 1200 °C and 1450 °C followed these heat treatments. Characterizations of the powders were performed with XRD, FTIR, thermal analysis, density measurements and particle size determinations.

According to the XRD patterns, complete transformation to alpha form occurred in powders previously heat treated at 900 °C, mechanical treated and then calcined at 1200 °C in 8 hours and 1450 °C in 2 hours. Powders that were calcined at 1100 °C and 1200 °C in 1-2 hours contained considerable amount of kappa form together with alpha.

The effect of the polyethylene oxide-polypropylene oxide-polyethylene oxide (PEO/PPO/PEO) blockcopolymers on the dispersion behaviour of alumina powder suspensions in water were investigated at  $\Phi=0.125, 1.0, 14$  and 50 vol% solid loadings by rheological and turbidity measurements. To compare the effects of block copolymers with other type of dispersants, measurements of some other well known dispersants were also conducted at  $10^{-7}$  to  $10^{-3}$  M. The results indicated that type block copolymers with high EO percentage have a positive effect when they are used with ultrasonic treatment on the agglomerated alumina suspensions. But it was not able to create stable dispersions in the absence of ultrasonic bath application. Turbidity measurements at  $\Phi=0.5$  wt% showed that some dispersants gave higher dispersion but the stability was reached after a time period. Ultrasonic treatment created stability but lowered the turbidity values.

# CHAPTER I

## INTRODUCTION

Ceramics can be defined as inorganic and non-metallic materials or compounds. They have been produced for centuries. The earliest ceramic articles were made from naturally occurring raw materials. However during the past 50 years it was found that naturally occurring minerals could be refined or new compositions synthesized to achieve required properties.

Alumina ( $\text{Al}_2\text{O}_3$ ) is the most widely used oxide ceramic because it is plentiful, relatively low in cost and equal to or better than most oxides in mechanical properties [57]. The advanced ceramics generally require chemical conversion of raw materials into intermediate compounds, which lend themselves to purification and subsequent chemical conversion into the final desired form.

In general ceramic materials undergo reconstructive transformation. They transform by nucleation and growth with high activation energies. For ceramic fabrication it is necessary to transform the ceramic powder to the stable form before consolidation as low densities are usually obtained on sintering if the ceramic powder undergoes transformation during heating. However because of the elevated temperatures imposed by the high activation energy the ceramic powder becomes coarsened, aggregated and generally unsuitable for ceramic processing and fabrication without subsequent processing [50, 30]. Nucleation and growth of these powders that undergo transformation during calcination may be affected by parameters and techniques such as seeding, mechanical treatment, and thermal treatment environment.

Many researchers had studied the transformation to metastable alumina forms starting from different aluminium hydroxides. Also a number of researchers have attempted to influence the transformation to alpha alumina by using additives such as  $\alpha\text{-Al}_2\text{O}_3$ , CuO, MgO,  $\alpha\text{-Fe}_2\text{O}_3$ ,  $\alpha\text{-Cr}_2\text{O}_3$ . Seeding of a

transition alumina with these additives accelerates the kinetics of transformation and prevents formation of a vermicular microstructure [51,37,30,10,32,49,39].

A mechanical pre-treatment (compaction or dry ball milling) of transition alumina powders significantly affects the kinetics of the transformation and very high compaction pressures ( $>2.5\text{Gpa}$ ) can prevent the formation of a vermicular microstructure characterized by the coexistence of contiguous solid and pore phases [32].

The recent studies generally involve importance of seeding of the transition form aluminas before transformation to alpha alumina. Especially mechanism of gamma to alpha transformation has been subject of several published studies. On the other hand a few studies [9] have been observed about mechanical treatment to improve nucleation and growth of  $\alpha$ -alumina. Also there was no attention on the effect of ultrasonic treatment on nucleation and growth rate of alumina. Previous studies related with the effects of both seeding and mechanical treatment on phase transformations will be discussed with more detail in Chapter II.

In ceramic processing after the powder preparation with suitable properties it is important to treat these powders before the consolidation step. Generally ceramic powders need a pre-consolidation step before the forming process. That is, in all kinds of forming techniques homogenisation of the powders by the help of all different chemical aids are necessary. Especially in some forming techniques like slip casting and tape casting usage of these chemical aids such as dispersing agents has a major importance for successful consolidation process. On this manner, in ceramic applications, for the preparation of alumina powder suspensions to create an effective dispersion and stabilization, usage of some different dispersing agents maybe required.

There are many studies that investigate the effect of different type of dispersants such as polyacrylic acid, polymethacrylic acid, citric acid, sodium dodecyl sulfate, benzoic acid derivatives, anionic and cationic surfactants on the dispersion and stabilization behaviour of alumina [6,11,12,19,24,53].



An alternative dispersant for alumina suspensions might be the polyethylene oxide-polypropylene oxide- polyethylene oxide (PEO/PPO/PEO) type block copolymers. Because they are effective over a wide pH range, wide structural variations make them effective for a variety of particle types and their high molecular weight provides effective steric stabilization [4]. There are many studies related with dispersion and adsorption behaviours of these polymers on many materials [1,13,16,38]. However there is very little information on the use of these polymers with alumina.

In this study, the objective was to prepare the fine alumina powders starting from Bayer gibbsite and obtain stable alumina suspensions in water by using PEO/PPO/PEO tri block copolymers.

During the powder preparation, thermal decomposition of gibbsite was achieved. It was attempted to increase the transformation rate to alpha alumina by mechanical treatment process like ball milling and use of ultrasonic bath. For the alumina suspension preparation, a tri block copolymer was preferred because they are important class of surfactants and find widespread industrial applications that include dispersion stability. Hence it was intended to investigate their effect on alumina particles in water.

## CHAPTER II

### ALUMINA

Many of the raw materials used in the ancient times are still used today and form the basis of the ceramic industry. These ceramic products are often referred to as traditional ceramics. The clay minerals are the main source for the production of these ceramics.

On the other hand, new ceramics, which are produced by refined or synthesized, are referred to as advanced ceramics. They include the oxide ceramics such as  $\text{Al}_2\text{O}_3$ ,  $\text{ZrO}_2$ ,  $\text{MgO}$ , etc. Among other oxides, alumina ( $\text{Al}_2\text{O}_3$ ) is the most widely utilized one. It has a major importance as a raw material for the production of both traditional and advanced ceramics.

#### 2.1 Structure and Transition Forms

There are many poly-types of alumina. Alpha alumina with hexagonal type of corundum structure is the most thermally and chemically stable one. Alumina has a mixed ionic and covalent bond structure. It has a low formation energy and high melting point as  $2050^\circ\text{C}$ . Its single crystals are transparent [37].

Alumina has some intermediate, metastable forms. Haber in 1925 divided the alumina into two series, which is alpha and gamma that depends upon their calcination temperatures. The symbol alpha was applied to the more abundant form in nature and calcined at higher temperature [57].

The name gamma was given to an undescribed alumina by Ulrich in 1925. This term has been used in many cases for all the alumina transition forms occurred in the low temperature calcination of alumina. Then it was restricted

the name gamma to the product obtained in the dehydration sequence of gibbsite and boehmite at 500 °C [57].

As new forms have been identified, they have been assigned Greek letters. These transition phases are denoted as  $\chi$ (chi),  $\eta$ (eta),  $\epsilon$ (epsilon),  $\delta$  (delta),  $\theta$ (theta),  $\gamma$ (gamma),  $\beta$ (beta) and  $\kappa$ (kappa). Some additional monoclinic  $\text{Al}_2\text{O}_3$  forms have been identified recently as  $\theta'$ ,  $\theta''$ ,  $\kappa'$  and  $\lambda$  [32]. All of these metastable forms have partially disordered crystal structures based on a close packed oxygen sub-lattice with varying interstitial aluminum configurations. As equilibrium is approached the structures become more ordered until stable alpha alumina is formed.

The crystal structure of alpha alumina is often described as having  $\text{O}^{2-}$  anions in a hexagonal closed packed arrangement with  $\text{Al}^{+3}$  cations occupying two thirds of the octahedral interstices [28, 57, 32, 34].

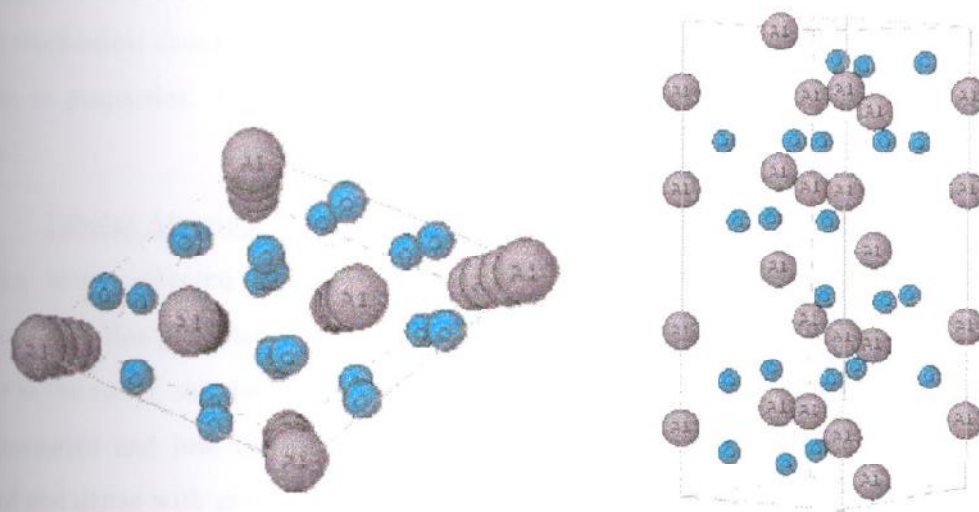


Figure 2.1. Crystal structure of alpha alumina.

All the metastable aluminas can be divided into two broad categories; a face centered cubic (fcc) and hexagonal closed packed (hcp) arrangement of oxygen anions [32].

The alumina structures based on (fcc) packing of oxygen include  $\gamma$ ,  $\eta$  (cubic),  $\theta$  (monoclinic) and  $\delta$  (either tetragonal or orthorhombic) [32, 35].

While usually treated as cubic, gamma alumina has a slightly tetragonally distorted defect spinel structure ( $c/a$  about 0.99, the distortion varying with heat treatment). Also delta alumina has a tetragonal super structure [34]. On the other hand alumina structures based on the (hcp) packing are presented by  $\alpha$  (trigonal),  $\kappa$  (orthorhombic) and  $\chi$  (hexagonal) forms.

## 2.2 Types and Applications

Five types of alumina are generally considered for use in ceramic products: [14, 35, 57]

Activated Alumina: It is highly porous (about 200-400 m<sup>2</sup>/g surface area) with granular form of alumina. This type of alumina generally used as a catalyst, catalyst carriers and adsorbent. It exhibits high resistance to thermal and mechanical shock and abrasion. Also it can hold moisture without change in form or properties. The crystalline structure is normally chi, eta, gamma and rho.

Tabular Alumina: They are nearly 100% alpha phase. The conversion to alpha being affected by heating the material above 1870°C. The large, hexagonal, elongated tablet shaped alpha alumina crystals characterize and give rise to the name 'tabular alumina'. They are used especially in alumina graphite refractories and low cement refractories mixes. Tabular alumina crystals are hard and dense with good thermal conductivity and high crushing strength [34].

Fused Alumina: Melting calcined alumina at above 2040 °C in an electric arc furnace produces them. It is produced in 2 forms: white and brown. White fused alumina is made from calcined Bayer alumina. Brown fused alumina is made from bauxite ore under conditions that allow only partial removal of impurities such as ferrosilicon [34].

Calcined Alumina: They are available in many grades based on the degree of calcination and Na<sub>2</sub>O content (< 0.01 to nominally 0.5%). Fully calcined aluminas are primarily alpha phase. Calcined aluminas have the



hardness and durability character. There are 4 main uses of calcined aluminas. In the production of fused alumina, in the production of ceramics with high alumina content, as an additive material such as in refractory, as a polishing material [25].

Colloidal Alumina: It is an aqueous dispersion of nanometer sized alumina particles. The alumina particles are treated with an acid to produce a positive surface charge, which causes the particles to repeal each other.

The important characteristics of alumina are the thermal resistivity, high hardness and electrical insulation and also the chemical stability. In addition to these its production process and the economic cost are the other factors within its advantages. However it has some limitations such as low toughness, poor thermal shock resistance and low temperature strength.

Alumina is also very important raw material in the production of traditional ceramics such as grinding media, wear resistant tiles, insulators, dinnerware, seals, and valves. In the high temperature engineering applications there are pipes, plates and jigs for high temperature uses, transparent tubes for sodium lamps, wear resistant parts like wire guides and nozzles, mechanical seals and cutting tools. In electrical applications it is used as spark plug insulators, electronic substrates, electrical insulation. In addition to these, because of their fine particle size, high surface area and catalytic activity of their surfaces, the transition alumina finds applications in industry as adsorbents, coating, soft abrasives, catalyst or catalyst carriers [32].

### **2.3 Alumina Production Methods**

The powders which are used in advanced ceramics manufacturing such as alumina are generally in sub micrometer size range and tend to have a quite narrow size distribution to ensure rapid and uniform sintering leading to uniform grain size in the final product [46].



On the other hand abrasives must be available in many sizes. Refractories generally require a bimodal or multimodal particle size distribution. Many different powder synthesis, sizing, purification techniques have been developed to achieve the various required distribution. Today a great number of these techniques are available, differing widely in the characteristics of the produced powders, as well as in parameters such as yield and cost of production [47].

Important amount of the alumina production in the world is made from bauxite with the exception of few operations. Production methods are completely chemical and consist of only extraction of alumina from its impurities. Main types of alumina production methods can be grouped as:

**Electrothermal Method:** In this method mixture of the ore and the reducing material is melted in an electrical furnace so that impurities are reduced and melted alumina is obtained. Examples are Pedersen Process, Hall Process.

**Sinter Method:** This method can be applied both for the bauxites with high silica content and some type of clays. In this process the feed should contain necessary amount of sodium and potassium oxide for the conversion to alumina, limestone and nepheline.

**Acidic Method:** It is based on the principle of treatment of the ore with mineral acid solutions such as hydrochloric acid.

**Basic Method:** This method depends on the reaction of bauxite with NaOH and  $\text{Na}_2\text{CO}_3$ . At the end of the reaction, aluminium oxide dissolves and the soluble sodium aluminate is obtained. Bayer Process is an example of this method [25].

### 2.3.1 Bayer process

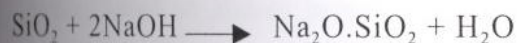
Bayer process is applied to the ores with low silica content. In other words this process is applied to high quality bauxites which contains more than 50% alumina and less than 15% silica. It consists five primary operations: Raw material preparation, digestion, clarification, precipitation, and calcination.

The first step involves crushing, blending and grinding of bauxite. In the process the ore is ground in ball mills with sodium hydroxide. Sometimes some lime is added to the mixture for caustification. Aim of this is to recover NaOH from harmful  $\text{Na}_2\text{CO}_3$ .

Digestion step requires the dissolving of alumina from bauxite in a caustic soda solution under heat and pressure. During that operation most of the alumina goes into solution as sodium aluminate. In this step following reactions occur in the system:



Digestion is performed in steel autoclaves or in tubular reactors at temperatures up to 250 °C, 30 atm. with caustic concentrations up to 190 g/l. The digest slurry is held at temperature for an additional 15-30 minutes to decrease the silica concentration of the liquor by formation of a sodium aluminium silicate, which is insoluble in any aqueous solution.



Clarification step involves the separating of undissolved mud from sodium aluminate liquor. Pulp coming from autoclaves includes sodium aluminate solution and the insoluble residues known as red mud. Iron, silica and titanium from the bauxite remain insoluble and are removed by settling and filtration. But impurities like  $\text{V}_2\text{O}_5$ ,  $\text{Cr}_2\text{O}_3$  and  $\text{P}_2\text{O}_5$  get into solution. This mud

may have a very fine particle size. The fine solids behave as relatively stable colloidal suspensions so some flocculants such as starch are added.

Precipitation requires hydrolysis of the sodium aluminate. To carry out precipitation, aluminate liquor is seeded with the fines and the mixture is agitated. The seed grows to crystal agglomerates that are easy to separate and wash [25].

The filters feed large rotary kilns or fluid bed calciners where the obtained aluminium hydroxides are heated to 1100–1200 °C. By calcination hydrated alumina, is turned to anhydrous alumina. The types of hydrated aluminas obtained from bauxite in some cases by Bayer process and also their decomposition sequences will be discussed in the following headlines.

## 2.4 Aluminum Hydroxides

Alumina occurs in nature as impure hydroxides. These are the essential constituents of bauxite ores. Bauxite, is an impure mixture of boehmite, diaspor which are the  $\alpha$  and  $\beta$  forms of  $\text{AlO}(\text{OH})$ , respectively and also other hydroxides.

Gibbsite (hydrargillite) is  $\alpha\text{-Al}(\text{OH})_3$ . It is a naturally occurring mineral but the Bayer process can be used to produce it. The oxygen ions in the gibbsite structure form close-packed layers with aluminium cations sandwiched in octahedrally coordinated interstices between the layers [32]. Grains of gibbsite precipitated in Bayer process are aggregates of tabular and prismatic crystals. Gibbsite usually contains some alkali metal ions. The highest alkali concentrations are found in technical trihydroxide produced by the Bayer process. It was showed that sodium is atomically dispersed in the crystal lattice of gibbsite.

Most of the technical trihydroxide is used as an intermediate in the manufacture of aluminium. Other industrial uses are white pigment, filler for



paper, fireproofing and reinforcing agent for plastics and rubber and as a raw material for the preparation of aluminium compounds [57, 32].

Bayerite, that is  $\beta\text{-Al(OH)}_3$ , is rarely found in nature but it can be prepared in the laboratory. The oxygen coordination in the bayerite structure is similar to that in gibbsite, but the distribution of hydrogen atoms is different [32]. It is produced commercially, principally for catalysts and applications requiring high purity aluminum hydroxides.

Boehmite, that is  $\alpha\text{-AlO(OH)}$ , is the major constituent of bauxite minerals and also it can be produced in the laboratory. For example by neutralizing aluminium salts at temperatures close to the boiling point of water. Heating pseudoboehmite results in the formation of transition alumina in a sequence similar to that associated with bayerite.

Samples of boehmite usually contain water in excess of the theoretical 15%. This water is probably bound as  $\text{Al(OH)}_3$ , as judged by the temperature, kinetics and heat requirements of its decomposition. But some authors do not accept this hypothesis and consider the excess water as intercrystalline.

Diaspore,  $\beta\text{-AlO(OH)}$  occurs in nature. The structure consists of hexagonal layers of oxygen [34]. The oxygen ions are nearly equivalent, each being joined to one other oxygen by way of a hydrogen ion and being arranged in hexagonal close packing. Since diaspore is usually associated with older bauxite, high pressure and elevated temperatures is necessary for the formation [57]. But also it can form at ambient temperatures and pressures.

## **2.5 Phase Relations of Aluminum Hydroxides and Oxides**

Technical aluminum oxide is prepared by calcining gibbsite up to  $1300^\circ\text{C}$ . During heating the hydroxide undergoes a series of structural changes that yield technically valuable properties of the partially calcined product, such as high surface activity and large specific surface area [57]. The variables of the calcination process and the structures of the transition forms between the stable

hydroxides and the alpha alumina have been studied extensively during the past 50 years.

### 2.5.1 Thermal Decomposition of Aluminum Hydroxides

In many investigations the transformation of hydrous and transitional oxides of aluminum have been conducted with systems in which the nucleation step has not been controlled. These transformations have been widely characterised in terms of pore development.

Decomposition sequence of alumina is strongly dependent on the starting material and how it is processed. For example, if the starting material is boehmite then the most probable sequence is gamma ( $\gamma$ ), delta ( $\delta$ ), theta ( $\theta$ ) and alpha ( $\alpha$ ). On the other hand, if the starting material is gibbsite, the sequence may include chi ( $\chi$ ), kappa ( $\kappa$ ) and alpha ( $\alpha$ ). Another polymorph that is diasporite transforms directly to alpha alumina. During the transformation of all these aluminas, highly porous microstructure is developed [34].

Moreover, the sequence of transformation is not reversible when the temperature is decreased. In other words, neither alpha alumina nor the other high temperature forms can be converted to alumina that occur at lower temperatures. Hence they may be classified thermodynamically stable. At partial pressures of water vapour far below saturation and in the absence of mineralisers, a series of transformation occur that is demonstrated in Table 2.1.

Wilson and Stacey [59] studied these aluminium oxide phases derived from boehmite. According to them, the dehydration of crystalline boehmite is topotactic and produces  $\gamma$ -alumina. The subsequent transformation to  $\delta$  and  $\theta$  alumina is also topotactic (that is, changes in crystal structure are accomplished without changes in crystal morphology).

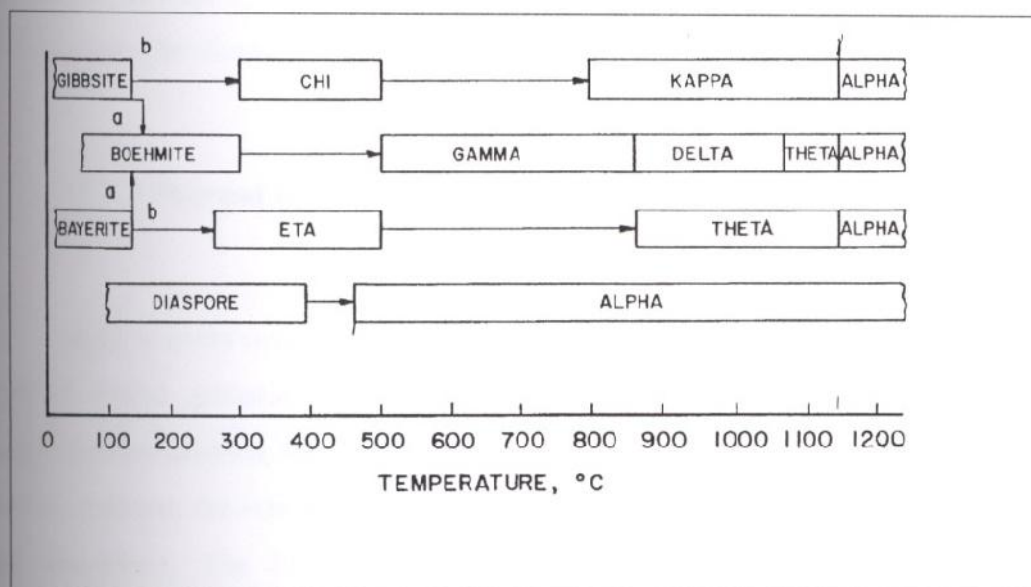
According to Levin et al. [32] the sequences of the phase transformations reported in the literature on passing from the metastable alumina structures to the final stable  $\alpha$  alumina are approximate. This means, no direct experimental

evidence has confirmed the existence of a direct  $\delta$  to  $\theta$  transformation or disproved a direct  $\gamma$  to  $\alpha$  transformation. Published experimental results suggest that the  $\gamma$  to  $\alpha$  transformation is not direct.

Table 2.1. Transition sequences of aluminum hydroxides [57].

Path a: > 1 atm.- moist air, > 1°C/min., particle size >100 $\mu$ m

Path b: 1 atm.- dry air, < 1 °C/min., particle size < 10  $\mu$ m



Also according to the same authors it is possible to reach alpha alumina starting from tohdite. This conversion is followed by the following mechanism,

5  $\text{Al}_2\text{O}_3 \cdot \text{H}_2\text{O}$  (Tohdite) convert to  $\kappa'$  at (700-800 °C) will followed by  $\kappa$  at (850 °C) and it will convert to  $\alpha$  at 900 °C.

Iler [23] studied the conversion of boehmite to transition aluminas and  $\alpha$  alumina. For this purpose starting materials were fibrillar colloidal boehmite, finely divided boehmite in the form of thin elongated platelets and macroscopic boehmite crystals. In the range 500 to 700 °C boehmite was converted to fibrillar  $\gamma$  (gamma) without unchanged in size. At about 1000 °C it yielded  $\theta$  (theta)- alumina. Finally in the range 1000 to 1100 °C all the aluminas were converted to alpha.



Levin and Brandon [32] noticed that the transformation from fcc-based transition aluminas to alpha alumina often proceeds by nucleation and growth of individual single crystals of alpha alumina, with an internal porous vermicular-like microstructure, characterized by the coexistence of contiguous solid and pore phases. The development of a vermicular microstructure has been found to be a major obstacle inhibiting the pressureless sintering of nanosized transition alumina powders at low temperatures ( $< 1300\text{ }^{\circ}\text{C}$ ). They also mentioned that the characterization of vermicular microstructure has received little attention, and no detailed attempt to analyse the morphology and the crystallography of this structure has been found in the literature.

#### **2.5.1.1 Thermal Decomposition of Gibbsite**

Many workers investigated the relationships between the specific surface area of heated gibbsite and variables of calcination. There is a general agreement that absolute figures depend on the purity and the particle size of the starting material, the rate of the heating and the vapour pressure of the water in the atmosphere. The Figure 2.2 illustrates the relationships between the temperature, specific surface area, density and loss on ignition of calcined gibbsite. Since the process is accompanied by an increase in density from 2.42 to  $3.98\text{ g/cm}^3$  a large internal surface area is created. Neither weight loss nor surface area is linear functions of temperature and time of calcination.

Dehydroxylation and change in density create a network of sub microscopic cracks in the heated gibbsite crystal. The internal surface area reaches a maximum at calcination temperatures between  $300\text{-}400\text{ }^{\circ}\text{C}$ . The initial step in the thermal decomposition of hydroxides is the diffusion of protons that react with  $\text{OH}^-$  ions to form  $\text{H}_2\text{O}$ . This process removes the binding forces in the gibbsite structure and changes the chemical composition. The layers break up into many areas of short- range order [57].

Most investigators agree that boehmite and a disordered transition alumina are formed upon heating of coarse gibbsite at about  $400\text{ }^{\circ}\text{C}$ . Calcination

of fine crystalline gibbsite, especially at low water vapour pressures, leads to the transition form only. Some researchers believed that this transition alumina is the  $\chi$ -chi form. The stacking sequence of the layers of  $\chi$ -alumina is strongly disordered. When fine-grained gibbsite is rapidly heated to about 300 °C under high vacuum an amorphous product, that is rho- alumina is obtained.

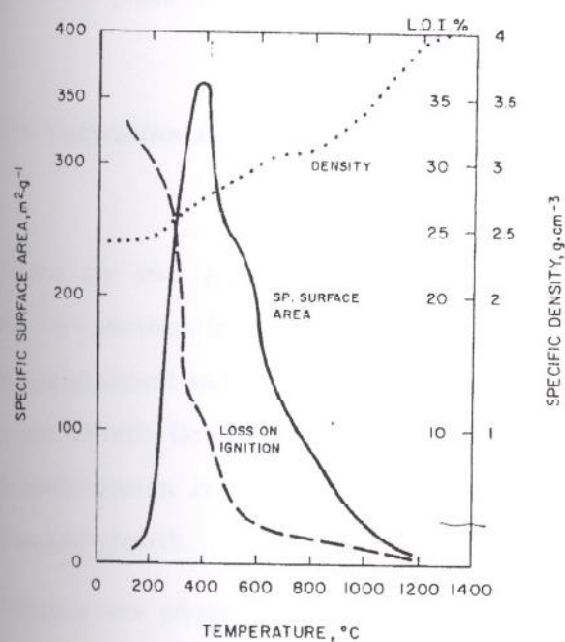


Figure 2.2. Relations between some properties of calcined gibbsite [57].

In 1958 it was distinguished two types of pores in the transition to  $\chi$ -alumina. Between 225 and 250°C pores of about 30 °A were formed by the initial release of water resulting in surface area of 60 m²/g. As the dehydration proceeded, a second system of slit shaped pores developed having diameters of 10°A and additional surface area of 200 to 250 m²/g. This texture was retained throughout the transition to alpha alumina. Surface area rises to a peak as 350 m²/g for one-hour calcination at 400 °C in dry air. It was pointed out that the highest surface area occurred at a composition of  $\text{Al}_2\text{O}_3 \cdot 0.5\text{H}_2\text{O}$  for many atmospheres, temperatures and times of heating [57].

X-ray diffraction patterns of samples heated above 800 °C indicate a better-ordered transition form,  $\kappa$ -alumina. It has a loss on ignition of 1 to 2 %.

Only after prolonged heating above 1100 °C this value reduced 0.1 to 0.2 %. According to the Table 2.1,  $\kappa$ -alumina transforms to  $\alpha$ -alumina at about 1150 °C in dry air, 1 atm. with  $< 1^\circ\text{C}/\text{min.}$  heating rate.

With the loss of practically all OH ions, the anion lattice of kappa is better ordered than that of the low temperature  $\chi$ -form. In addition, a reordering of cations takes place in the transition  $\chi$  to  $\kappa$ -alumina [57, 32].

## 2.6 Nucleation and Growth

There are two general types of processes by which one phase can transform into another. In the first type changes are initially small in degree but large in spatial extent and in the early stages of transformation. In the other type changes are initially large in degree but small in spatial extent. The first type of phase transformation is called spinodal decomposition and the latter termed nucleation and growth.

When a new phase is formed by nucleation and growth process, it must start in a very small region and then increase in size. Nucleation from a homogeneous phase is called homogeneous nucleation. However when the surfaces, grain boundaries, second phase particles and other discontinuities in the structure serve as favourable sites, the process is called heterogenous nucleation.

After a stable nucleus has been formed it grows at a fixed rate by conditions of temperature and the degree of supersaturation. The rate of growth is determined by the rate at which material reaches the surface and the rate at which it can build into the crystal structure [29].

The transformation from faced centred cubic (fcc) based transition aluminas to alpha alumina derived by calcination of various salts and hydroxides often proceeds by nucleation and growth of the individual single crystals of alpha alumina with an internal porous vermicular like microstructure, associated with the large volume change accompanying the transformation [32].



### 2.6.1 Effects of Seeding

The concept of seeding in order to enhance the kinetics and to control the development of the desired phase has been widely used in the synthesis of ceramics [51]. Seeding of a transition alumina with  $\alpha$  alumina particles accelerates the kinetics of transformation and prevents formation of a vermicular microstructure. They are shown to act as nuclei for transformation and to result in an increase in the transformation kinetics and lowering transformation temperature. Seed concentration, seed matrix dispersion and size are critical parameters for successful control of the transformation. Many authors have added a variety of potential nucleation aids such as  $\alpha$ - $\text{Al}_2\text{O}_3$ , CuO, MgO,  $\alpha$ - $\text{Fe}_2\text{O}_3$ ,  $\alpha$ - $\text{Cr}_2\text{O}_3$  to alumina gels. The effect of these “seeds” is primarily dependent on the similarity of the crystal structure to  $\alpha$ - $\text{Al}_2\text{O}_3$ .

Messing and co-workers [37] have demonstrated the controlled transformation and sintering of boehmite prepared by sol-gel in the presence of  $\alpha$ -alumina seeding. According to their studies addition of  $\alpha$ -alumina particles per  $1 \text{ cm}^3$  of  $\gamma$ -alumina could effectively seed the alpha alumina phase transformation. The transformation temperature decreased as  $170^\circ\text{C}$  with seeding and the incubation time was reduced from hours to a few minutes. In addition to these effects the refinement and reduction of alpha alumina sintering temperature to below  $1200^\circ\text{C}$  was more important. They attributed the temperature reduction for the sintering to the avoidance of the development of the characteristic vermicular microstructure, microstructural refinement and reduction of diffusion distances.

Wakao and Hibino [29] added a number of different oxides up to 10 wt% to an aluminium sulphate derived  $\gamma$ -alumina and they reported that the temperature of the  $\theta$  to  $\alpha$ -alumina transformation was reduced in all cases, with CuO and  $\text{Fe}_2\text{O}_3$  lowering the transformation temperature to as low as  $1050^\circ\text{C}$ . Bye and Simpkin added chromium and iron via a solution technique to  $\gamma$ -alumina powder. They showed that the transformation temperature was lowered to  $995^\circ\text{C}$  with 5% Fe but Cr additions had no effect.

Kumagai and Messing [30] added 1.5 wt%  $\alpha$ -alumina to pseudoboehmite gels and found the  $\alpha$ -alumina crystallization peak temperature was reduced from 1215°C to 1075°C. Similarly, hematite ( $\alpha$ -Fe<sub>2</sub>O<sub>3</sub>) seeds lower the crystallization peak because hematite has the corundum crystal structure. Additives with a crystal structure very different from  $\alpha$ -alumina tend to have less significant or no effects on the transformation to  $\alpha$  alumina.

Dynys and Halloran [10,51] added the equivalent of 0.4 wt% MgO,  $\alpha$ -Fe<sub>2</sub>O<sub>3</sub> and  $\alpha$ -Cr<sub>2</sub>O<sub>3</sub> via water-soluble salts to aluminium secbutoxide derived boehmite. They showed  $\alpha$ -Fe<sub>2</sub>O<sub>3</sub> enhanced the transformation kinetics while  $\alpha$ -Cr<sub>2</sub>O<sub>3</sub> and MgO additions had no effect in transition. Also they have reported a nucleation density of  $10^8 \text{ cm}^{-3}$  for an alum derived  $\gamma$ -alumina. The reason for the strong influence of seed concentration is due to the degree of grain refinement (volume per seed) by controlled transformation. The effects of seed concentration and seed/matrix dispersion probably explain why they did not observe an effect on the  $\alpha$  alumina transformation when they added  $\alpha$  -alumina particles to an  $\gamma$ -alumina powder.

Shaklee and Messing [3] used HF as a mineraliser for the transformation of  $\gamma$  to  $\alpha$ -alumina. They proposed that vapour transport by AlF<sub>3</sub>O increased the transformation rates. The transformation to alpha alumina was complete after 30 minutes at 900 °C when optimum reactant concentrations were used.

In another work, the influence of different additives on the kinetics of the phase transformation has been studied. According to this study, less than 1 wt% of additive did not change the sequence of the polymorphic transformation during dehydroxylation of aluminium trihydroxide, but it has been observed that the promotion of  $\alpha$ -alumina formation is accompanied by destabilization of  $\theta$ -alumina. The influence of the additives on the transformation has been related to the respective radii and then charge of the specific cations. The additives promote  $\alpha$ -alumina formation for differences in ionic radii between the host and foreign cations of < 33%, whereas a difference in the radii of >33% stabilize the less dense  $\delta$  or  $\theta$ -alumina forms [32].

Saito et al. [49] studied the effects of various  $\text{SiO}_2$  phases on the  $\gamma$  alumina to  $\alpha$ -alumina phase transition. According to their results by adding amorphous  $\text{SiO}_2$  such as fumed silica was considered to retard the transition by preventing particles from coming into contact and suppressing heterogeneous nucleation on the  $\gamma$ -alumina surface. On the other hand addition of a crystalline  $\text{SiO}_2$  such as quartz and cristobalite, showed a different effect. They attributed the reason of acceleration of the  $\gamma$  to  $\alpha$  phase transition to the heterogeneous nucleation mechanism.

Bagwell and Messing [3] studied transformation kinetics and coarsening rates in unseeded and  $\alpha$ -alumina seeded  $\gamma$ -alumina powders heated in dry air and water vapour. According to their results altering both nucleation and growth process accelerated the transformation. Seeding the transformation with  $\alpha$  alumina effectively eliminated the barrier to nucleation. Also the presence of the water vapour accelerated diffusion in the system. Seeding with  $\alpha$ -alumina increased the transformation rates and reduced incubation times by providing low-energy sites for nucleation and growth of the  $\alpha$ -alumina transformation.

In another study influence of zirconium and magnesium dopants on the transformation from the transition aluminas to  $\alpha$ -alumina have been studied. The addition of magnesium cations enhanced the rate of the transformation from  $\gamma$  or  $\delta$  alumina in to the  $\alpha$ -alumina form, whereas the addition of zirconium cations inhibited the transformation. Also it was demonstrated that the presence of water vapour enhances the rate of the transformation [32].

The published results showed that additives can influence both the temperature and the rate of the gamma to alpha form transformation, and they can change the sequence of intermediate phases during transformation.



## 2.6.2 Effects of Mechanical Treatment

A mechanical pre-treatment like compaction or dry ball milling of transition alumina powders significantly affects the kinetics of the transformation. Dynys and Halloran studied the formation of  $\alpha$ -alumina in  $\gamma$  alumina, which is obtained from ammonium alum at 1150 °C.

According to their results, mechanical treatments of the gamma alumina markedly increased the density of the nuclei and the transformation rate. The nucleation density affects the final grain size by dictating the volume of transition alumina matrix. To determine the effect of mechanical pre-treatment, they compared the transformation kinetics of untreated powders with the kinetics of powders, which had been either compacted in a biaxial, die or dry ball-milled or both [9]. They reported that the nucleation frequency increased from  $10^8$  to  $10^{12}$  cm<sup>-3</sup> after ball milling the  $\gamma$ -alumina powder in an alumina ball mill with alumina media. They also demonstrated that the compaction of the  $\gamma$ -alumina powder prior to transformation increased the transformation kinetics. They carried out experiments to determine whether  $\alpha$ -alumina 'debris' or particles generated during milling may have increased the transformation kinetics, but it was concluded that the mill 'debris' was not responsible for the increased nucleation frequency.

According to the results the reason for the improvement of the nucleation rate may be enhancement by the creation of the new surfaces during milling. But the observation that the BET surface area was nearly unaffected by milling suggested that little new surface has been created. It was possible that this small new surface could provide potent sites for nucleation. A possible explanation for the increase in the nucleation frequency could be framed in terms of a break down of the foamy macrostructure of the calcined powder.

As a result they concluded that the mechanical pre-treatment apparently increases the rate of nucleation frequency of  $\alpha$ -alumina, but the mechanism remains uncertain. Nucleation of  $\alpha$ -alumina in  $\gamma$ -alumina precursor at a high compaction pressure may occur by shear of the atomic planes in the  $\gamma$ -alumina.

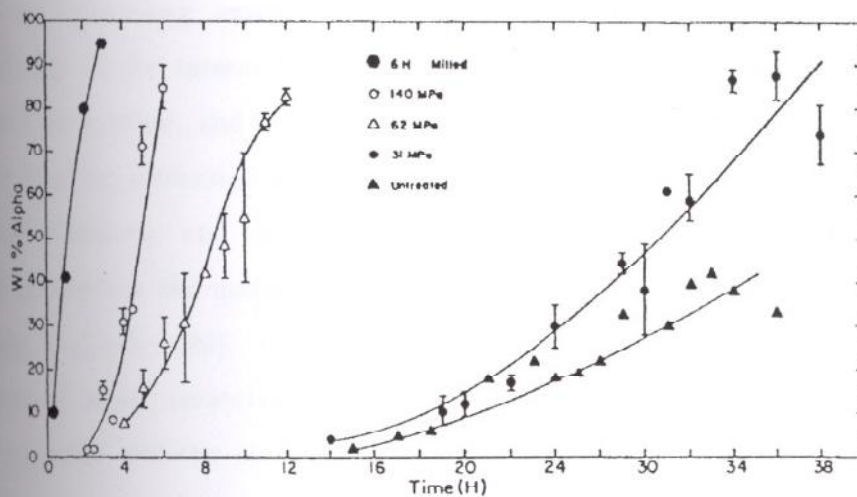


Figure 2.3. Formation of  $\alpha$ -alumina in untreated and die-pressed  $\gamma$ -alumina powders at 1150 °C [9].

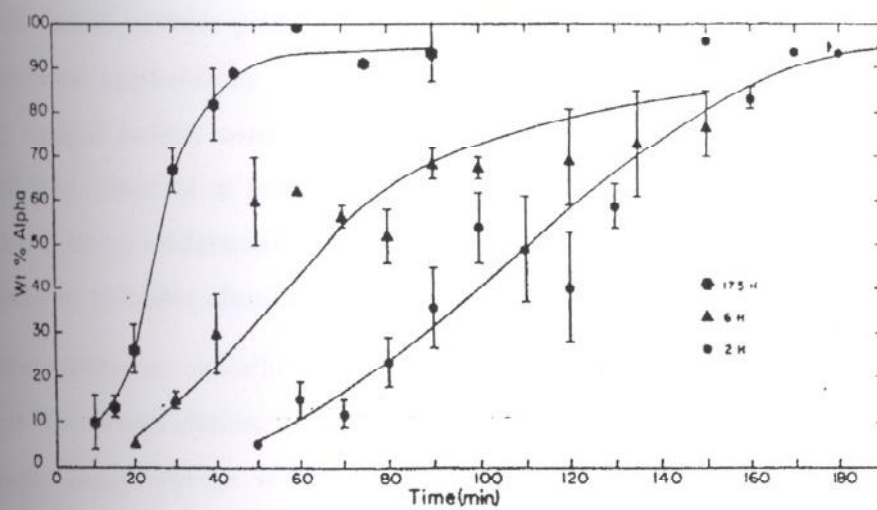


Figure 2.4. Formation of  $\alpha$ -alumina in ball milled  $\gamma$ -alumina powders annealed at 1150 °C [9].

## 2.7 AQUEOUS ALUMINA SUSPENSIONS

Colloidal processing of advanced ceramic powders such as alumina has received an increasing amount of attention in recent years [17]. A clear understanding of the interactions between the particles dispersed in aqueous media with each other, and with the surrounding phase has a great importance for those who are interested in the outcome of such processes as flocculation, dispersion, flotation, etc. An understanding of these interactions therefore essential to improve the quality of the alumina ceramics produced by colloidal processing methods [20]. In other words, key factors for the successful production of these ceramics are the homogenisation and dispersion of the powder particles and the stability of the suspension. In general, the goal in colloidal processing of ceramic powders is to achieve homogeneous suspensions with high solid loading and defined rheological properties [21].

Alumina powder dispersions in liquids are normally very unstable because the small powder particles have tendency to create agglomerates [35]. So in ceramic applications of this powder, a pre-consolidation step may generally require before consolidation of this powders to specified shape. At this point it is essential to give some information about ceramic consolidation techniques to better understanding of importance of the colloidal processing and the preparation of stable alumina dispersions.

Many different consolidation techniques are used in industry. They are divided as dry consolidation, that is pressing; plastic forming or consolidation with dough; consolidation with slip, that is casting [35]. Major compaction techniques are listed in Table 2.2.

Slip casting and pressing are the major consolidation techniques in the production of alumina ceramics. Feed having a slurry consistency may be formed by the casting technique. In slip casting, the slurry is poured into a porous mold. Capillary section of the mold absorbs liquid from the slurry and particles that consolidate on the surface of the mold form a cast. Pressure or vacuum may be applied to increase the casting rate [50,47,43,34]. Since slip



## CHAPTER III

### EXPERIMENTAL

#### 3.1 Materials

Bayer gibbsite and transition alumina used in this work were obtained from Seydişehir Aluminum Company. Gibbsite was reported to have a chemical composition of 64%  $\text{Al}_2\text{O}_3$ , 0.3%  $\text{Na}_2\text{O}$ , 0.015 %  $\text{Fe}_2\text{O}_3$ , 0.015%  $\text{SiO}_2$  and 80% of the powder with above 40  $\mu\text{m}$  particles. The transition alumina was reported to have a composition of 98,5%  $\text{Al}_2\text{O}_3$ , 0.5%  $\text{Na}_2\text{O}$ , 0.025 %  $\text{Fe}_2\text{O}_3$ , 0.020%  $\text{SiO}_2$  with minimum 25%  $\alpha$  phase.

Two commercial high purity  $\alpha$ -  $\text{Al}_2\text{O}_3$  powders were used in this study. The first powder (AKP-53) has an average particle size of 0.29  $\mu\text{m}$ , a BET surface area of 12.3  $\text{m}^2/\text{g}$ , bulk density (tapped) of 1.5  $\text{g}/\text{cm}^3$  and loose bulk density of 1.1  $\text{g}/\text{cm}^3$ . The powder purity exceeded 99.99%, containing 140 ppm Si, 7 ppm Na, 20 ppm Mg, < 1 ppm Cu and 9 ppm Fe. This powder and above information was kindly supplied by Sumitomo Chemicals Co., Japan. The second powder with an average particle size of below 10  $\mu\text{m}$  was purchased from Aldrich Chemicals Co.

The pH of the 20 vol% AKP-53 and Aldrich alumina suspensions was measured as 5.96 and 9.33 at 33°C respectively in distilled water without additives. The pH of the gibbsite suspension was measured as 9.36 at 26°C. In the case of transition alumina suspension the pH was measured as 9.8 at 23°C.

PEO/PPO tri block co-polymers (commercially known as Pluronic) were obtained from BASF Corporation, Washington, NJ. Structural formulas of block copolymers used in this study were indicated in Chapter II Figure 2.13. Their important properties and compositions are further listed in Table 3.1 and 3.2 respectively.

Table 3.1. Important properties of surfactants used in this study [2].

Code	Mol. weight	%PEO	Melt pour point ©	viscosity (cps)77°C
F-127.....	12600.....	70.....	56.....	3100
F-68.....	8400.....	80.....	52.....	1000
P-104.....	5900.....	40.....	32.....	390
PE-6400.....	2900.....	40.....	16.....	850
10R-8.....	4550.....	80.....		

Table 3.2. Compositions of surfactants used in this study [56].

F-127.....	EO <sub>97</sub> PO <sub>69</sub> EO <sub>97</sub>
F-68.....	EO <sub>78</sub> PO <sub>30</sub> EO <sub>78</sub>
P-104.....	EO <sub>13</sub> PO <sub>30</sub> EO <sub>13</sub>

Polyacrylic acid (with an average molecular weight  $M_w$  of 2000) from Aldrich, citric acid with  $M_w$ : 192 (Merck) and sodium dodecyl sulphate  $M_w$ : 288 (Sigma) were also used as dispersing agents at concentrations ranging from  $10^{-7}$  to  $10^{-2}$  M.

Distilled water used during the experiments had a conductivity of 113.5  $\mu\text{S}/\text{cm}$  (24.6 °C) obtained from equipment Jencons Autostills DDI/C.

### 3.2 Powder Preparation Methods

Alumina powders were prepared from gibbsite by using eight different methods in this work. The processing steps for the first four methods are shown in Figure 3.1. The purpose of these variations in the processing steps was to influence the nucleation and growth rate of the solid-solid phase transformations. The powders were coded all at the end of the processing diagrams.

Gibbsite was wet ball milled for 16 hours in the first four methods. Multifix Ball mill was used with a plastic container with 4.9 cm radius and cylindrical zirconia media of 9.48 mm height. During milling, bulk volume was calculated by the summation of the ball volume and the void volume between the grinding media. The powders were ground at 115 rpm (85% of the critical speed).

The ball-milled gibbsite was further heat treated at 350 °C for 4 hours in methods 1 and 2. The particle size determination of the powders after milling was performed by using Stoke's law,

$$[V = (g_s - g_f) \rho x^2 / 18\mu]$$

Where;

$g_s$ : Density of the solid

$g_f$ : Density of the fluid

$\rho$ : 9.81 m/s<sup>2</sup>,  $x$ : particle size,  $\mu$ : viscosity of the fluid

Settling time of the particles in the suspension was calculated by using terminal velocity that was obtained from the above equation at a specified height. The pH of the suspensions were adjusted to 3.5 with nitric acid to avoid agglomeration during sedimentation. Fractionation of the powders was accomplished by letting the suspensions for a preset time and separating the sediment and the suspension. Fractions below 1  $\mu\text{m}$  and 5  $\mu\text{m}$  from the powders were recovered and used for further processing.



Powders smaller than  $1\text{ }\mu\text{m}$  particle size were calcined at  $1200\text{ }^{\circ}\text{C}$ , for 2 to 8 hours in a high temperature furnace (Carbolite 1600 RHF, with  $5^{\circ}\text{C}/\text{min}$  heating rate). The final powders were designated as M-1A and M-1B respectively. The powder labelled as M-1P in method 1 was ball milled for 9 more hours. The  $< 5\text{ }\mu\text{m}$  powder fraction was calcined at  $1100\text{ }^{\circ}\text{C}$ , for 2 hours under similar conditions.

The powder M-3 was prepared without heat treatment at  $350\text{ }^{\circ}\text{C}$ . Gibbsite was milled for 16 hours and the  $< 5\text{ }\mu\text{m}$  fraction of the powders was calcined at  $1200\text{ }^{\circ}\text{C}$  for 2 hours.

In the preparation of powder M-4, the transition alumina was used as the starting material. It was ball milled and fractionated. The  $< 5\text{ }\mu\text{m}$  fraction was calcined at  $1200\text{ }^{\circ}\text{C}$  for 2 hours. Powder processing steps of powders M-1, M-2, M-3 and M-4 were presented in Figure 3.1.

M-3

M-4

Figure 3.1.

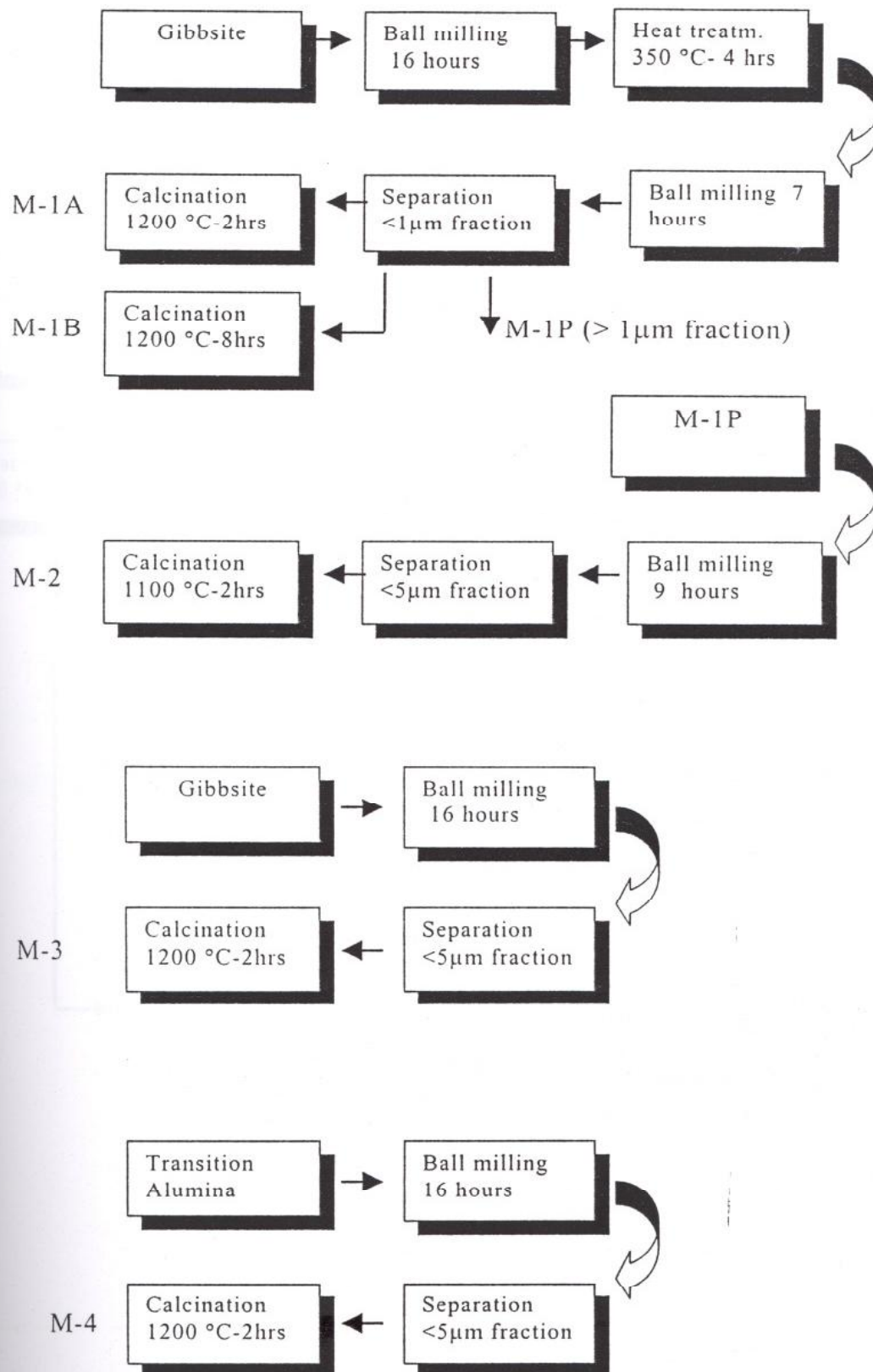


Figure 3.1. Powder processing diagram of M-1, M-2, M-3 and M-4.

Gibbsite was directly heat treated at 900 °C for 3.5 hours in methods 5 to 7 (M-5 to M-7) as indicated in Figure 3.2. The effect of ball milling and ultrasonic treatment was investigated on the transition to alpha alumina transformation.

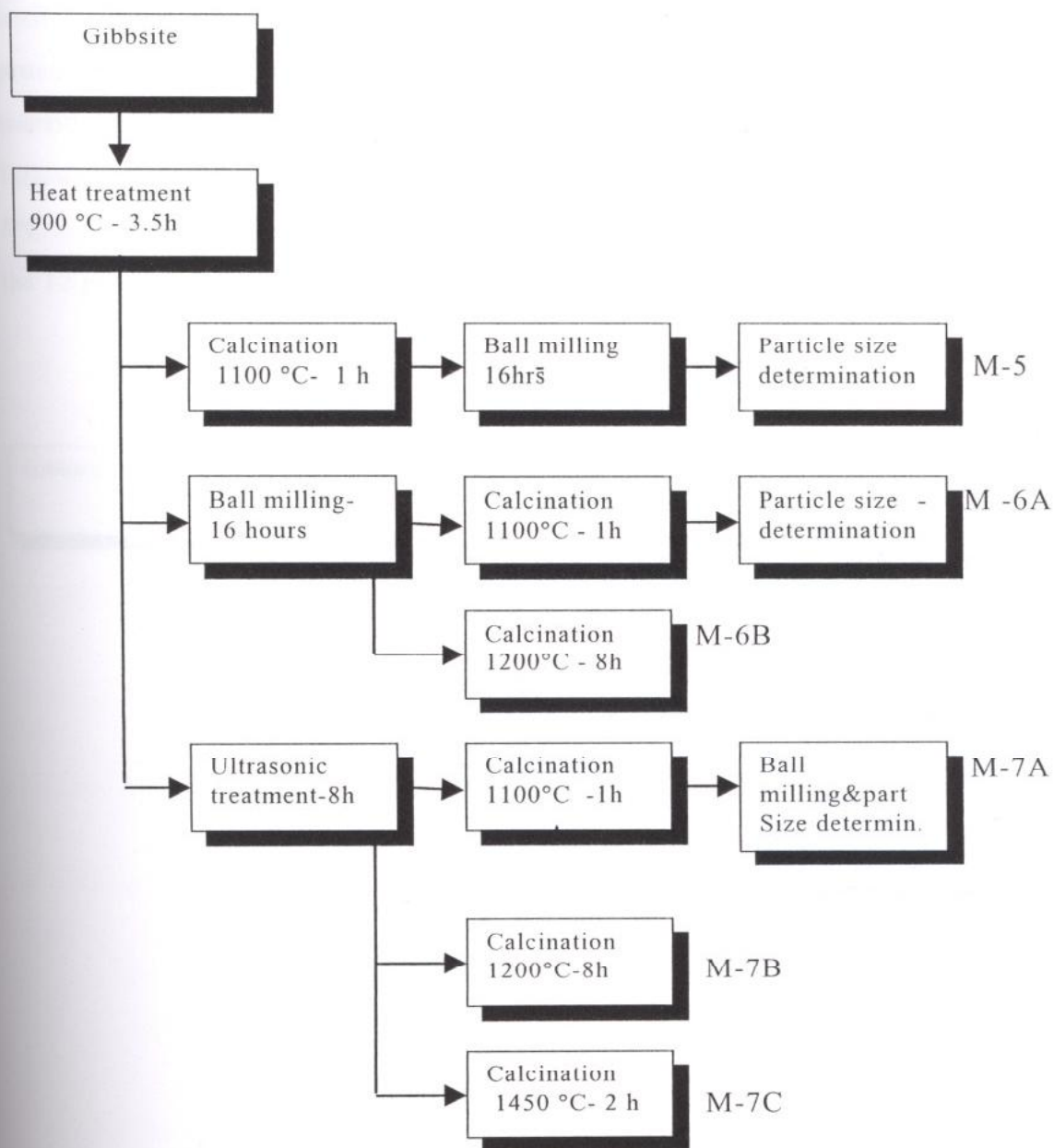


Figure 3.2. Powder processing diagram of M-5, M-6 and M-7.



In the preparation method of powder M-8, gibbsite was primarily ball milled for 5 hours that was followed by heat treatment at 350°C for 4 hours. The secondary ball milling was also performed for 5 hours with 1 hour ultrasonic treatment. For this purpose Elma Transsonic 660/H (35 kHz) ultrasonic bath was used. During ultrasonic treatment, samples were also stirred to enhance the process. Then powders were thermally treated at 900 °C to transform to a transition alumina. The third ball milling and ultrasonic treatment process followed this. Finally powders were calcined at 1100 °C for 1 hour with 5°C/min and ball milled after calcination. The powder preparation steps of all the 12 powders are further tabulated in Table 3.3.

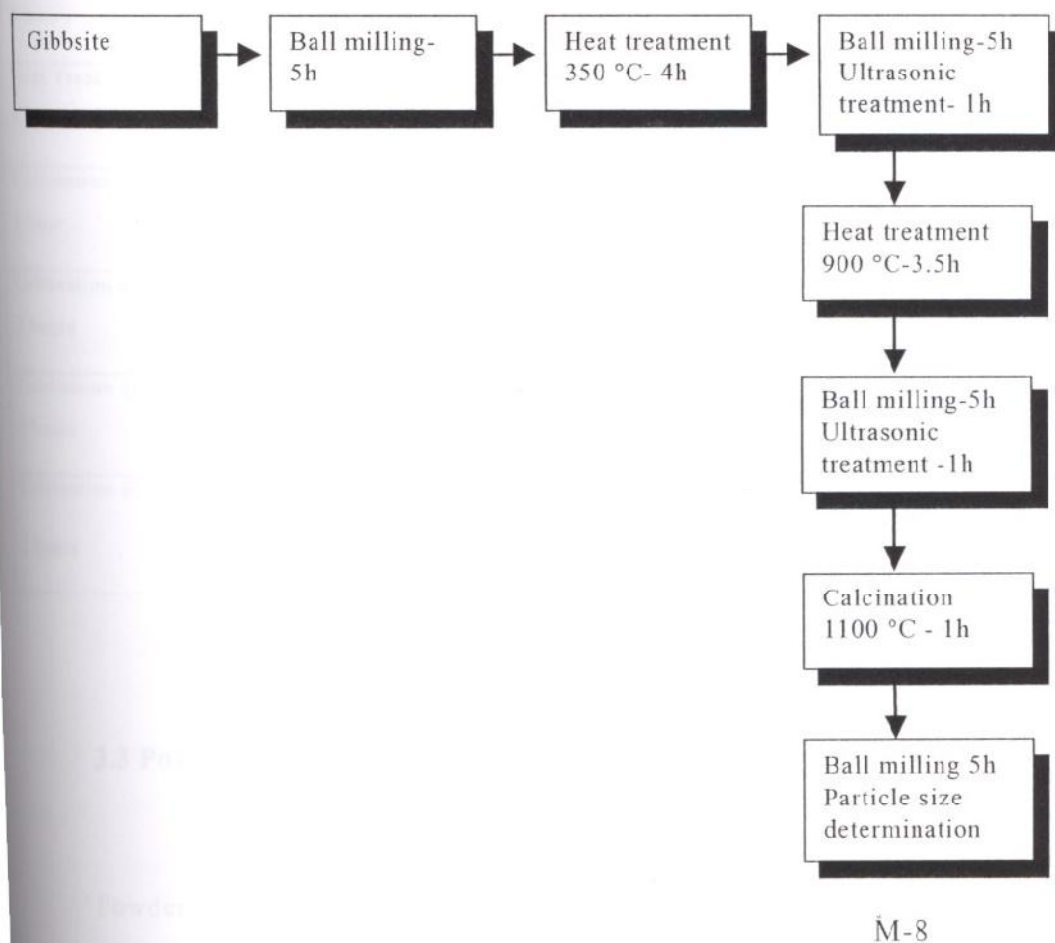


Figure 3.3. Powder processing diagram of M-8.

Table 3.3. Processing methods of prepared powders.

Powder Preparation Methods	M-1 A	M-1 B	M-2	M-3	M-4	M-5	M-6 A	M-6 B	M-7 A	M-7 B	M-7 C	M-8
1 <sup>st</sup> Grinding (Before heat treatment)	●	●	●	●	●							●
2 <sup>nd</sup> Grinding (After heat treatment)	●	●	●				●	●				●
Final Grinding (After calcination)						●			●			●
Ultrasonic Treatment									●	●	●	●
Heat Treat. @ 350 °C 4 hours	●	●	●									●
Heat Treat. @ 900 °C 3.5 hours						●	●	●	●	●	●	●
Calcination @1100 °C 1 hour			●			●	●		●			●
Calcination @1200 °C 2 hours	●			●	●							
Calcination @1200 °C 8 hours		●						●		●		
Calcination @ 1450°C 2 hours											●	

### 3.3 Powder Characterization

Powders with 3% PVA and 5% moisture were die pressed at 75 MPa by hydraulic hand press. Pellets were sintered at 1450°C for 2 hours in a high temperature furnace (Carbolite 1600 RHF). The sintered densities of the pellets

were determined by Archimedes method using a Sartorius BP 2108 with suitable density measurement apparatus.

Particle size distributions of the two commercial powders were determined by Mastersizer S.Ver.2.14, Malvern Instruments. Particle size information of the prepared powders were estimated and reported as a fraction of the total powder by use of Stoke's Law.

Thermal properties were examined by the Thermogravimetric Analyser (TGA- 51/51 H, Shimadzu Co.) at 1000°C with 10°C/min heating rate by using nitrogen as a carrier gas and Differential Thermal Analyser (DTA-50, Shimadzu Co.) at 1450°C.

The Infrared Spectra of the powders were taken by Fourier Transform Infrared Spectroscopy (FTIR-8201, Shimadzu Co.). The pellets for the FTIR analysis were prepared by pressing a mixture of the 0.004 gr samples and the 0.2 gr KBr.

The phase identification in selected samples was determined by powder X-ray diffractometer (Jeol JSDX 100S4) by using monochromatic  $\text{CuK}\alpha$  radiation with Ni filter. The  $2\theta$  was taken 6-80° with 2°/min scanning rate and 20 mm/min chart rate (In Dokuz Eylül University, Mining Engineering Department).

### **3.4 Suspension Preparation Methods**

Suspensions were prepared by using AKP-53, Aldrich alumina and the powder M-7A. Solid loadings in suspensions were adjusted as 0.125, 1.0, 14, 50 vol % respectively (0.5, 4, 40, 80 wt %) for the viscosity measurements and only 0.5 wt % for turbidity measurements. Suspensions were prepared by using different methods. These are as follows (Figure 3.4.):



## CHAPTER IV

### RESULTS AND DISCUSSION

#### 4.1 Powder Preparation and Characterization

Powders that were prepared with the methods mentioned in previous chapter were characterized with XRD, FTIR, density measurements and particle size characterizations. The thermal behaviour of the gibbsite was also determined. Results will be discussed in the following paragraphs.

##### 4.1.1 Thermal Analysis

Differential thermal and thermogravimetric analysis of gibbsite in Figures 4.1 and 4.2 showed that most of the hydroxyl ions are driven off below 400 °C. In this study some of the powders were thermally treated at 350 °C to obtain high surface area powder with a network of sub microscopic cracks. According to Wefers [1972] there are two endothermic peaks below this temperature in the DTA curve of a coarse grained gibbsite. The first one appears near 230 °C .It is followed by an exothermic effect at approximately 280 °C, attributed to the formation of boehmite by hydrothermal conditions due to the retarded diffusion of the water vapour out of larger grains. The exothermic reaction does not occur in DTA curves of the fine-grained trihydroxide [57]. Most investigators agree that boehmite and a disordered transition alumina (chi) are formed upon heating of coarse gibbsite to about 400 °C.

In this study there are three regions in the TGA curve of the gibbsite (Figure 4.1). The first stage between 250-330 °C is due to the decomposition of the hydroxide and the removal of water vapor. The total weight loss is about 25% in this stage.

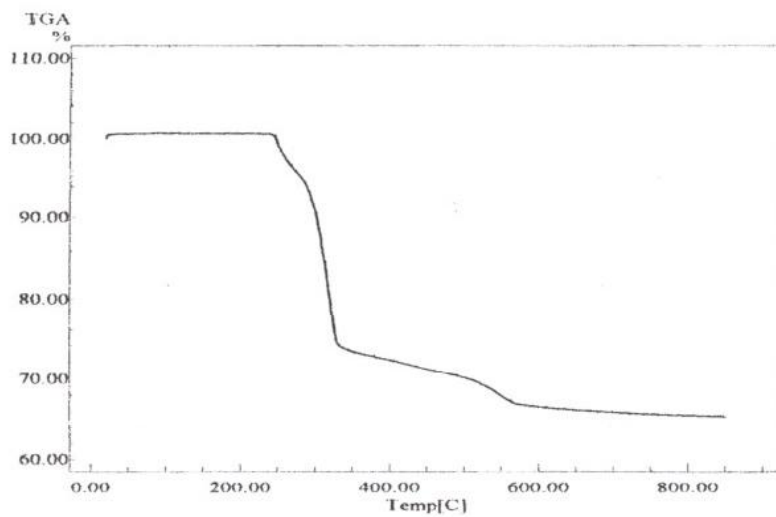


Figure 4.1. TGA thermogram of gibbsite.

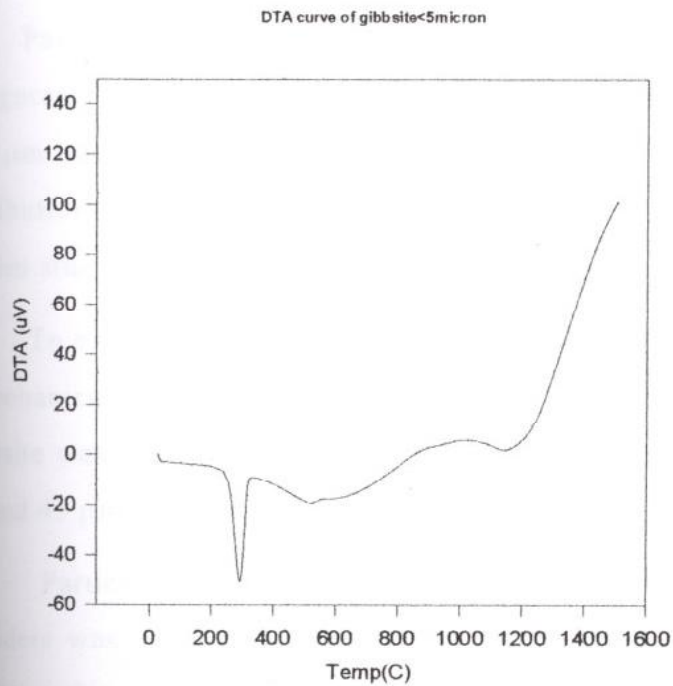


Figure 4.2. DTA curve of gibbsite.

In the DTA curve of the gibbsite there is an endothermic peak at 300 °C (Figure 4.2). This endothermic peak is located in the same temperature range as stage I in the TGA curve and can be attributed to the gibbsite decomposition.

The second stage, which is between 330-510 °C in the TGA curve, may be due to diffusion of the trapped water in the structure. The last stage, which is between 510- 550 °C, may be due to the decomposition of the boehmite formed in the first stage. There is also an endothermic depression in DTA curve in that temperature range similarly attributed to the decomposition of boehmite. In the third stage of the TGA curve weight loss is more rapid than the second stage but in quantity as 2 %. The total weight loss in the gibbsite was observed as

#### **4.1.2 Particle Size Characterizations**

Particle size distributions of the AKP-53 and Aldrich alumina were given in Figures 4.3 and 4.4 respectively. The reported particle size of the AKP-53 is 0.5  $\mu\text{m}$  but the Figure 4.3 demonstrated rather coarse particle size. Since size distribution measurements were taken without the use of ultrasonic bath in the present study this difference was attributed to the existence of agglomerates.

To examine the particle size of the gibbsite dry sieving was applied with mechanical vibrator during 60 minutes. According to the results 49.7 % of the sample was above 75  $\mu\text{m}$ , 16.8% was below 45  $\mu\text{m}$  and 33% was between the 45  $\mu\text{m}$ .

Particle size of the gibbsite used in the preparation of M-1 to M-3 samples was calculated after 16 hours grinding. Fractionation of the ground sample showed that 15.7% was below 1  $\mu\text{m}$  and 42% was below 5  $\mu\text{m}$ . After the first treatment that was followed by second grinding 14.3% of the gibbsite was determined to be below 1  $\mu\text{m}$  and 70% was below 5  $\mu\text{m}$ . The purpose of the treatment process at 350 °C was to obtain a disordered structure, which



may help the size reduction during grinding process. But relatively low percent of submicron fraction was obtained. The particle size of the transition alumina used in the preparation of M-4 was measured by dry sieving. Below 45  $\mu\text{m}$  fraction of the powder was 34.2%. In the case of M-4 powder after grinding for 16 hours below 5  $\mu\text{m}$  fraction was determined as 41.5 %.

In the case of M-5, 30.8% of the powder was smaller than 1  $\mu\text{m}$  after final calcination and 16 hours grinding step. For the powder M-6A this value was obtained as 21% and 68% of the powder was < 5  $\mu\text{m}$ . But the grinding step was before the calcination in the case of M-6A. The difference between the < 1  $\mu\text{m}$  fractions of the M-5 and M-6A was attributed to the processing step of grinding. The grinding process that was applied after calcination step was more efficient in size reduction.

The below 1  $\mu\text{m}$  fraction of the powder M-7A was determined as 45 % after calcination but it was 30.8% in the case of M-5. The only difference between the M-5 and M-7A was the usage of ultrasonic bath in the case M-7A. So it may be thought that usage of ultrasonic treatment before calcination may affect the particle size and the nucleation rate of the transition alumina.

In the case of M-8 below 1  $\mu\text{m}$  fraction was obtained as 10%, which was the lowest value. Some agglomeration problem during fractionation might cause to obtain such a low value. Additional grinding process after calcination was eliminated this effect and below 1  $\mu\text{m}$  fraction was obtained as 69%. These results were also tabulated in Table 4.1.

Table 4.1. Below 1  $\mu\text{m}$  and 5  $\mu\text{m}$  fractions of some selected powders in different processing steps.

Powders	After 1 <sup>st</sup> Grinding (%)	After 2 <sup>nd</sup> Grinding (%)	Before Calcination (%)	After Calcination (%)
M-1A < 1 $\mu\text{m}$	15,7	14,3	-	-
M-1A < 5 $\mu\text{m}$	42	70	-	-
M-4 < 5 $\mu\text{m}$	-	41,5	-	-
M-5 < 1 $\mu\text{m}$	-	-	-	30,8
M-6A < 1 $\mu\text{m}$	-	-	21	-
M-6A < 5 $\mu\text{m}$	-	-	68	-
M-7A < 1 $\mu\text{m}$	-	-	-	45
M-8 < 1 $\mu\text{m}$	-	-	10	69

### 4.1.3 Density Measurements

In this study, densities of the powder pellets in green and sintered form were measured. Results were tabulated in Table 4.2 and show the average of three different measurements.

The sintered density of the AKP-53 powder pellet was measured as 3.87 g/cm<sup>3</sup> with 97% theoretical density (TD). This value was taken as a reference to compare the densities with other powders.

The sintered densities of the pellets prepared by powders M-1A and M-2 were measured as 3.46 and 3.15 g/cm<sup>3</sup>, respectively. On the other hand, density of the powder M-3 was lower than M-1A and M-2. The only difference between these powders was the absence of the thermal treatment at 350 °C in the preparation step of M-3.

The powders M-5, M-6A and M-7A were all prepared through heat treatment at 900 °C. The highest sintered density was obtained in powder M-7A as 3.603 g/cm<sup>3</sup> with 91% of theoretical density. The powder pellet of M-5 has rather low density as 3.116 g/cm<sup>3</sup>. The ultrasonic treatment that was applied to M-7A was absent in the powder M-5. So the rather high density of the M-7A might be attributed to the ultrasonic treatment effect. The sintered density of the powder pellet M-6A was determined as 2.935 g/cm<sup>3</sup>. This powder was ball milled before calcination to improve the transformation. But grinding before calcination to enhance the nucleation and growth rate did not influence the sintered density M-6A powder pellets. For the powder pellet of M-8 although ultrasonic treatment was applied sintered density was not high as M-7A. Theoretical density was calculated as only 77%.

#### 4.1.4 Fourier Transform Infra-Red (FTIR) Analysis

The bands that were observed between 400 to 850  $\text{cm}^{-1}$  were due to Al-O stretching. Especially Al-O peak at 740  $\text{cm}^{-1}$  exists in all powders. In the case of gibbsite this peak was observed at 741  $\text{cm}^{-1}$  [57].

In all cases there was an unassigned peak at 813  $\text{cm}^{-1}$ . For the powder M-1P there were some additional unassigned peaks at 960, 1080  $\text{cm}^{-1}$ . This powder also contained OH bending peak at 1650  $\text{cm}^{-1}$ . The powder M-8 showed OH bending peak at the same point.

According to D.H. Lee et al. [31] the infra-red bands at 3624-3620, 3527 and 3460  $\text{cm}^{-1}$  along with a doublet at 3396 and 3328-3383  $\text{cm}^{-1}$  are related with gibbsite type species.

In Figure 4.5(a) the FTIR spectrum indicates that the material is a hydrate. The strong and broad absorption bands are located in the region approximately at 3100, 3378, 3430, 3620, 3518  $\text{cm}^{-1}$ . This absorption is associated with the OH stretching vibrations in molecular water [57]. FTIR spectrum for alumina AKP-53, Aldrich alumina does not show any distinct bands in these regions.

In powders M-1P, M-6, M-7, M-8 there was a carbonate peak at nearly 1400  $\text{cm}^{-1}$ . This may be caused by  $\text{CO}_2$  adsorption from the atmosphere.

Same authors [31] reported bands at 1520 -1570  $\text{cm}^{-1}$  and/or 1350-1410  $\text{cm}^{-1}$  on adsorption of  $\text{CO}_2$  on gamma-alumina surface. These bands were associated with bicarbonate, unidentate or bidentate carbonate species but their exact assignment was unclear. The presence of surface impurities plays an important role adsorbing such species. For example, presence of  $\text{Na}^+$  ion on the alumina surface enhances the ability of adsorbing  $\text{CO}_2$ . According to them, the infra-red bands at 3305, 1520-1580 and 1390  $\text{cm}^{-1}$  can be associated with the surface species which has a dawsonite-like structure in Bayer processed alpha alumina.  $\text{CO}_2$  and  $\text{Na}^+$  ions on the alumina surface, resulting in the formation of a dawsonite ( $\text{NaAl}(\text{OH})_2\text{CO}_3$ ) on their surface.



#### 4.1.5 X-ray Powder Diffraction Analysis

XRD analysis was performed in the range 6 to 80° 2 $\theta$  range in order to investigate the nature of the alumina phases in the final alumina powders. The XRD patterns of the 10 of the 12 powders along with the pattern of the commercial high purity alpha alumina AKP-53 powder are given in the Figures 4.6 to 4.8. The codes of the powders are indicated on the patterns. XRD peaks of only  $\alpha$  and  $\kappa$  phases of the alumina were detected in all the patterns. The 2 $\theta$  peak locations and spacings of these phases along with relative line intensities up to about 2 $\theta$  = 80° obtained from literature and they are further tabulated in Table 4.3 [57].

The commercial AKP-53 powder XRD pattern shows the presence of mostly sharp 12 alpha ( $\alpha$ ) peaks. The powder is in pure alpha ( $\alpha$ ) form with no kappa ( $\kappa$ ) or other transition alumina form.

Powders were calcined at three different temperatures in this work (1100, 1200 and 1450 °C). Only powder M-7C was heat treated at 1450 °C for 2 hours, which is a relatively high temperature for the transition alumina to alpha phase conversion. XRD pattern of the powder M-7C is given in Figure 4.10 indicates a phase pure  $\alpha$  alumina with relatively sharp  $\alpha$  peaks. There are also very weak 5 peaks and three these were assigned as  $\kappa$ . These peaks may also represent another impurity phase containing sodium. The transformation is mostly complete and the powder is high purity  $\alpha$ .

The powders M-7B, M-6B and M-1B although processed differently were calcined at 1200 °C for 8 hours. The XRD patterns of these are given in Figure 4.10 indicates that two of these powders are high purity  $\alpha$  powders. These powders were heat treated at 900 °C and mechanically treated before calcination at 1100 °C for 1 hour (M-7B ultrasonically treated and M-6B ball milled). Heat treatment at 900 °C seems to favour the phase transformation at 1200°C. The XRD pattern of the third powder (M-1B) showed that the presence of a multiphase structure. This powder was heat treated at 350 °C and subsequently ball milled and calcined at 1200 °C for 8 hours. The heat treatment for a shorter



time (2 hours) at 1200 °C with similar processing (M-1A Figure 4.8) yields a multiphase powder with significantly less sharp  $\alpha$  peaks.

The XRD patterns of the powders M-5, M-6A and M-7A (all calcined at 1100 °C) indicated that differences in processing do have some affects on the nucleation of the  $\alpha$  phase in the  $\kappa$  phase. Heat treatment of the gibbsite at 900 °C followed by calcination at 1100°C resulted in the formation of almost pure  $\kappa$  phase. Ball milling (M-6A) and ultrasonic treatment (M-7A) prior to calcination at 1100 °C caused partial transformation to the  $\alpha$  phase. The XRD patterns of these powders given in Figure 4.9 indicate the presence of multiphase powders.

The processing of the powder M-8 involves all the pre-treatment steps. The XRD pattern indicates an almost single-phase  $\kappa$  powder. This powder also as reported earlier had 69% of the particles finer than 1 $\mu$ m. The sintered density was also relatively low (77 % TD). The explanation for the behaviour of this powder is yet unclear.